

N71-20465

CASE FILE COPY

COLLISIONLESS SHOCKS IN PLASMAS

H.W. Friedman, L.M. Linson, R.M. Patrick
and H.E. Petschek

RESEARCH REPORT 363

December 1970

supported jointly by

HEADQUARTERS

NATIONAL AERONAUTICS AND SPACE ADMINISTRATION

Washington, D.C.

under Contract No. NASW - 2040

and

AIR FORCE OFFICE OF SCIENTIFIC RESEARCH

OFFICE OF AEROSPACE RESEARCH

UNITED STATES AIR FORCE

Arlington, Virginia 22209

under Contract No. F44620-70-C-0023

Project: 9752-02



EVERETT RESEARCH LABORATORY

A DIVISION OF AVCO CORPORATION

QUALIFIED REQUESTORS MAY OBTAIN ADDITIONAL COPIES FROM THE DEFENSE DOCUMENTATION CENTER; ALL OTHERS SHOULD APPLY TO THE CLEARING HOUSE FOR FEDERAL SCIENTIFIC AND TECHNICAL INFORMATION,

REPRODUCTION, TRANSLATION, PUBLICATION, USE AND DISPOSAL IN WHOLE OR IN PART BY OR FOR THE UNITED STATES GOVERNMENT IS PERMITTED.

ABSTRACT

A review of experimental and theoretical work on shock waves in plasmas where classical collisions are unimportant is presented. The role of dissipation and dispersion in determining shock structure is described and several mechanisms which can provide the required dissipation in collisionless plasmas are discussed. Observations of collisionless shocks produced in laboratory experiments as well as the Earth's bow shock occurring naturally in space are described. Criteria are given when a shock may be considered thin so as to be treated as a discontinuity for flow field calculations. Experimental and theoretical areas where more work is needed are pointed out.

TABLE OF CONTENTS

	<u>Page</u>
Abstract	iii
I. INTRODUCTION	1
II. THEORETICAL DISCUSSION	5
III. EXPERIMENTAL TECHNIQUES	15
IV. COMPARISON OF EXPERIMENT AND THEORY	19
V. EARTH'S BOW SHOCK	25
VI. SUMMARY	31
REFERENCES	33

I. INTRODUCTION

In plasmas, interactions between fluid elements can occur on a basis other than binary collisions between individual particles. Collective effects lead to plasma turbulence which produces dissipation scale lengths which can be far shorter than the ordinary collision mean free path. Therefore, shock phenomena, which depend on the interaction length, can be thinner than a mean free path. The study of shock structure and turbulent scale lengths is important in order to determine when a shock is thin enough to be treated as a discontinuity for flow field calculations. In addition, shocks which are thinner than a mean free path provide examples for studying mechanisms of collisionless dissipation.

The first suggestion of the existence of collisionless shocks was made by Gold (1955) to explain the phenomenon of "sudden commencements" which are small, rapid rises in the Earth's magnetic field occurring a day or so after a solar flare. The characteristic velocity of the cloud of protons which are emitted as a blast is estimated at 10^3 km/sec from the delay time of a day. The sharp rise of the magnetic field in a couple of minutes thus indicates that the front of the cloud which was compressing the Earth's field can be no thicker than 10^5 km which is far less than a collision mean free path of 10^8 km.

Research on collisionless shocks was further motivated by the coming of the space age which lead to the accessibility of in situ observations in the steady flux of collisionless plasma flowing from the sun, the so-called solar wind (Parker 1958), and by research on controlled thermonuclear fusion where high temperatures are required to achieve a sustained thermonuclear reaction. The possible existence of a collisionless shock standing off of the Earth's dipole field which acts as an obstacle to the solar wind was postulated independently by Zhigulev and Romishevskii (1960), Axford (1962), and Kellogg (1962) and confirmed by Ness, Scarce and Seek (1964) by direct observations using satellite probes. In the attempt to control thermonuclear fusion, it has been widely hoped that collisionless shocks, like their collisional counterparts, would transfer flow energy directly into ion thermal energy.

Collective interactions between fluid elements occur in a plasma as a direct consequence of the fact that the constituents, composed of ions and electrons, are charged fluids. Fluctuations in the densities and mean velocities of these charged species act as sources for long range electric and magnetic fields. For nonequilibrium plasmas, i. e. plasmas containing spatial inhomogeneities and/or non-Maxwellian velocity distribution functions, the approach to equilibrium often generates unstable fluctuations thus giving rise to turbulent electromagnetic fields. These turbulent fields

cause a random scattering of the plasma particles thus increasing their random velocity and producing dissipation on scale lengths which depend upon the particular instability involved.

The study of collisionless shock structure is more complicated than that of collision-dominated shock structure because a plasma contains a rich spectrum of small amplitude waves. Plasma waves with different wavelengths propagate with different wave speeds and thus remain near each other for only a short time giving rise to weak interactions. As a result, there exists in plasmas a state of weak turbulence which has no analogue in ordinary gasdynamics. In gases there are only nondispersive sound waves, hence waves of different wavelengths remain near each other for long times and produce strong interactions. Turbulence develops rapidly from laminar conditions with no distinct interim state as can exist in a plasma. Another consequence of the large number of plasma waves is that there are a variety of scale lengths associated with different aspects of the shock structure, such as the magnetic field change, electron heating, or ion heating.

Before proceeding further, we must define what we mean by a collisionless plasma shock. A simple definition of the collisionless property is that for a given shock structure the dissipation provided by classical collisions is less than the dissipation which is required to make the shock. By classical collisions we refer to ordinary momentum transfer collisions, e. g. coulomb collisions, as well as charge exchange and ionizing collisions. The principal forms of dissipation which will be discussed are resistivity and viscosity. For collisionless plasmas, thermal conductivity appears to be unimportant. Resistivity inhibits electrical currents which result from the relative streaming of electrons and ions whereas viscosity inhibits the relative bulk flow between two plasmas. Generally speaking, the former heats electrons while the latter heats ions. For collisionless plasmas these dissipative mechanisms are still present, however, they do not result from collisions in the classical sense but rather from the interaction of particles with turbulent wave fields.

In this review we hope to present a picture of the current state of experimental and theoretical understanding of the structure of collisionless shocks. This review will not be exhaustive, but will report on the significant observations which have been made and the theoretical ideas which appear to be relevant for explaining the observations. We shall concentrate entirely on shocks in magnetized plasmas where the magnetic field plays a decisive role in determining the shock structure. We omit any discussion of electrostatic shocks where only electric fields determine the shock structure.

In Section II a theoretical discussion is presented which provides a framework for understanding the experimental observations. Included are discussions of nonlinear wave theory, anomalous dissipation in a collisionless plasma, and critical Mach numbers. Section III presents a brief description of the principal laboratory experiments and their limitations. In Section IV we describe the observed features of laboratory shocks and

relate the observations to theoretical ideas. In Section V we present a description of the Earth's bow shock which stands in the solar wind. Section VI contains a summary of our current understanding of collisionless shock structure and points out some unresolved questions and areas where future research will be fruitful.

II. THEORETICAL DISCUSSION

The effect of a shock on the flow properties of a collisionless plasma is shown schematically in Fig. 1. The electron (or ion) particle density n , magnetic field B , and temperature $T = T_e + T_i$ (subscripts e and i represent electrons and ions respectively) are all increased across a fast shock while the flow velocity V is decreased. We are concerned here with the possible mechanisms which can lead to the formation of a shock with a thickness L_S which is small compared to a typical flow field scale. The jump conditions across the shock (de Hoffman and Teller 1950), and thus the shock structure, depend on several parameters: the Alfvén Mach number $M_A = V/C_A$ where C_A is the Alfvén speed [$C_A = B/(\mu_0 n m_i)^{1/2}$]; the angle θ between the flow direction and the magnetic field; and the ratio of thermal to magnetic pressure $\beta = 2\mu_0 nKT/B^2$. The upstream flow can also be characterized by an additional parameter, the ratio of electron gyro to plasma frequency, ω_{ce}/ω_{pe} , [$\omega_{ce} = eB/m_e$; $\omega_{pe} = e(n/\epsilon_0 m_e)^{1/2}$], but in almost all cases of interest this ratio is less than unity and does not appear to be critical for classifying shock structure.

There is no single theory which describes the whole problem since the parameter range is large and the dissipation processes involve turbulence which is difficult to treat analytically. We therefore study various aspects of this problem separately and as a result, our treatment will of necessity be somewhat fragmentary. It is interesting to note that in the first half dozen years of research since 1958, theoretical ideas were more abundant than observations, but in the last half-dozen years, observations of collisionless shocks occurring naturally in the solar wind and produced in laboratory experiments have tended to stimulate theoretical approaches.

The shock structure for low Mach number and weak dissipation is determined by dispersive effects. These effects lead to a non-monotonic rise across the shock at a scale determined by the wavelength at which small amplitude waves become dispersive. For higher Mach number non-classical dissipation in the form of turbulence becomes the dominant factor in determining shock structure. The turbulence results from one or more of the linear waves going unstable, and thus the turbulent scale may depend upon the particular instability. We will not discuss the entire range of turbulent dissipation but only some examples which have been observed or suggested by observations.

An important feature of collisionless shocks is the appearance of critical values for parameters in the sense that they define a demarcation between different processes. In particular, we shall see that there is an angle θ_c such that precursor waves cannot propagate upstream for $\theta > \theta_c$, a Mach number above which dissipation dominates over dispersive effects,

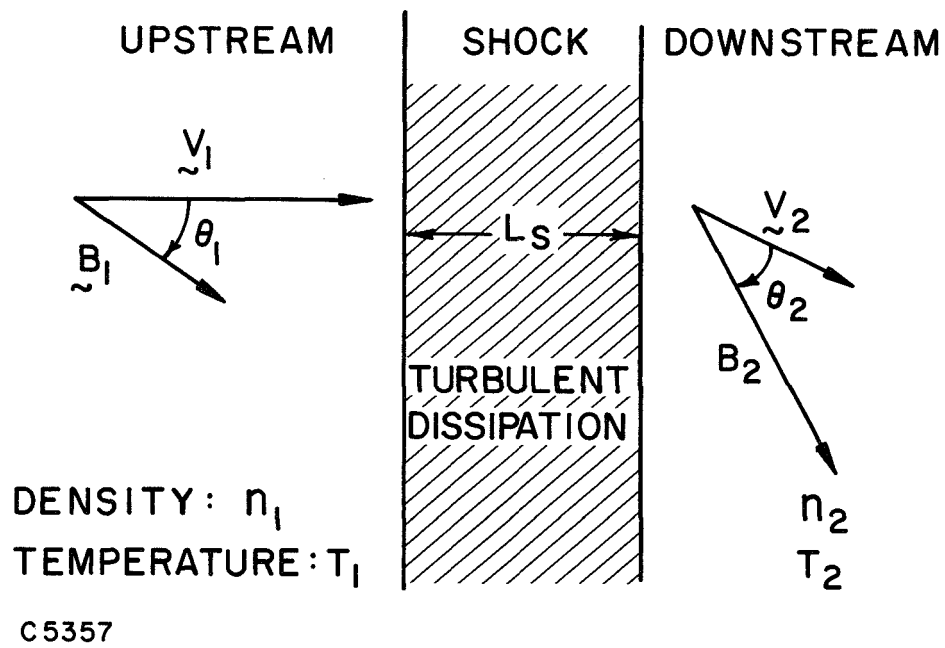


Fig. 1 Schematic of Collisionless Shock in a Magnetized Plasma

and a critical Mach number M^* above which resistive dissipation is insufficient to form a shock and a viscous-like dissipation is required.

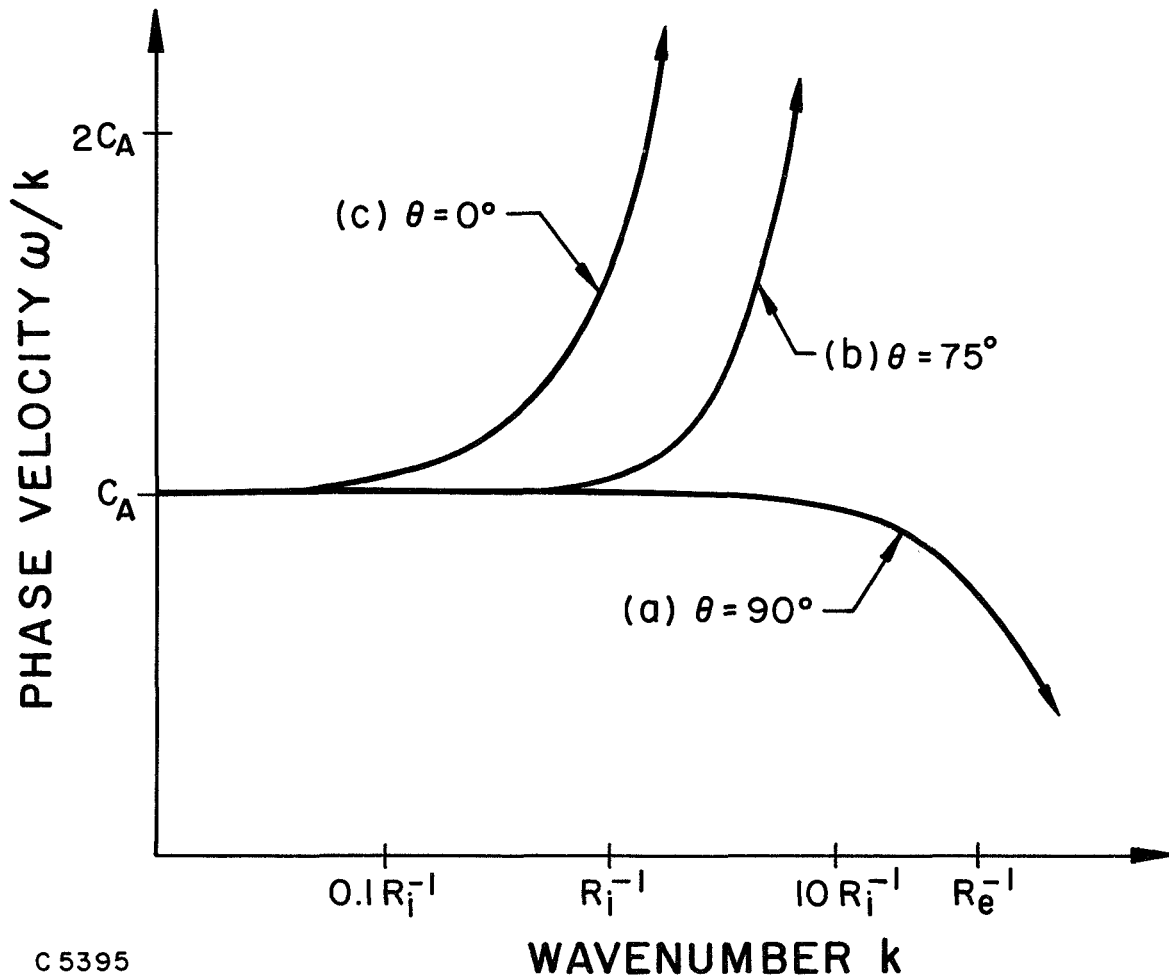
A. Dispersion Effects and Nonlinear Waves

Dispersion relates to the functional dependence of the frequency ω on wave number k for small amplitude waves. The spectrum of low frequency waves below the electron plasma frequency in a collisionless plasma has been derived and discussed by Stringer (1963) and Formisano and Kennel (1969) by treating the electrons and ions as separate fluids with equal densities and scalar pressures. Although we are working in a collisionless regime where fluid equations are not usually applicable, there are regions in parameter space where certain scale lengths less than a mean free path provide the basis for the use of fluid equations (Chew, Goldberger and Low 1956; Petschek 1958). In other regions of parameter space, e. g., near particle gyroresonances and wave numbers k_{\perp} such that $k\lambda_D \sim 1$ (λ_D is the Debye length C_e/ω_{pe} where $C_e = (KT_e/m_e)^{1/2}$ is an electron thermal velocity), the fluid equations are not adequate and a kinetic description is needed. However, the two fluid description has been quite successful in predicting the general properties of wave behavior in a plasma.

It is convenient to view shock waves as being formed from the steepening of a gradual pressure pulse. In ordinary gasdynamics a pressure pulse steepens by nonlinear effects until sufficiently steep gradients occur so that dissipative effects become important and a steady monotonic shock structure is achieved. Similarly, the magnetohydrodynamic (MHD) equations with collisional dissipative terms lead to the same phenomena as reviewed by Kantrowitz and Petschek (1966). In both of these cases the propagation speed of small amplitude waves is independent of wavelength and the only change in propagation properties that occurs at short wavelengths is dissipation. The two fluid equations are equivalent to the MHD equations for wavelengths which are long compared to $R_i = c/\omega_{pi}$, the speed of light divided by the ion plasma frequency. Hence steepening of a gradual pressure pulse is also to be expected in a collisionless plasma. However, at short wavelengths dispersion, not dissipation, limits the further steepening of a pressure pulse. Small amplitude waves are generated and carry energy either forward or backward depending on their dispersive properties. The result will be an oscillatory structure with either a leading or trailing wave train. A shock is formed when dissipation damps the wave train.

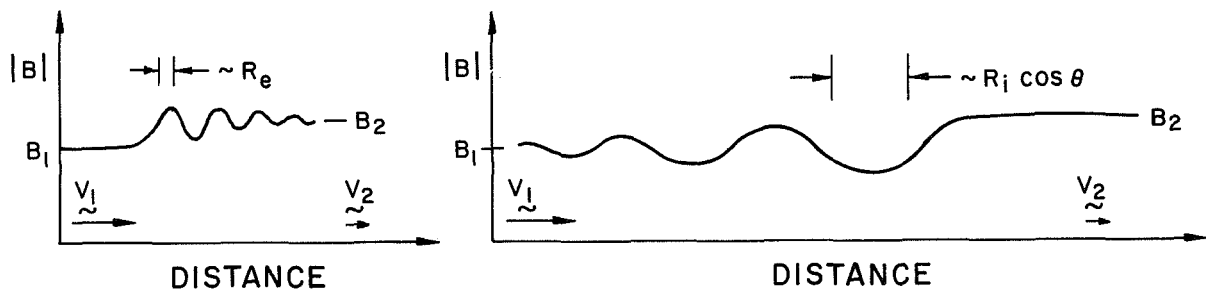
Figures 2 and 3 show specific examples of these effects for the fast wave mode propagating either perpendicular, obliquely or parallel to the magnetic field for a cold plasma. An expansion of the dispersion relation for the fast mode shown in Fig. 2 for small wave number k and nonparallel propagation results in

$$\frac{\omega}{k} \sim C_A \left[1 + \frac{1}{2} k^2 R_i^2 (\tan^2 \phi - \epsilon^2) \right] + O(k^4) \quad (1)$$



C 5395

Fig. 2 Phase Velocity of the Fast Mode Propagating (a) Perpendicular, (b) Oblique, and (c) Parallel to the Magnetic Field for $\beta = 0$ in Hydrogen



(a) Perpendicular

(b) Oblique

C5361

Fig. 3 Trailing and Leading Wave Trains Associated with (a) Perpendicular and (b) Oblique Propagation

where $\epsilon = (m_e/m_i)^{\frac{1}{2}} \ll 1$ and $\phi = \pi/2 - \theta$ is the angle between \underline{k} and the normal to \underline{B} . As a small amplitude wave steepens and generates shorter scale lengths, the higher order terms in k in Eq. (1) become important leading to waves which propagate either faster or slower than the original pulse depending on whether $\phi > \epsilon$ or $\phi < \epsilon$ respectively. Thus for perpendicular propagation ($\phi < \epsilon$) pulse steepening will lead to trailing wave trains when scale lengths reach the electron length $R_e = \epsilon R_i = c/\omega_{pe}$ while for oblique propagation ($\phi > \epsilon$) preceding wave trains can be expected when scale lengths approach $\phi R_i \sim R_i \cos \theta$ as indicated schematically in Fig. 3.

The MHD equations, and hence the two fluid equations, can support both fast and slow shock waves. Although slow shocks have long been hypothesized to exist (Petschek 1964; Petschek and Thorne 1967), there have only just recently been some reports of observations of slow shocks in the laboratory (Bratenahl and Yeates 1970) and in the solar wind (Chao 1970). Therefore we shall confine our attention here to fast shocks which have been studied extensively.

As a pulse steepens, linear wave theory breaks down and one must look for nonlinear solutions of the two fluid equations. These nonlinear solutions exist and have been studied extensively for cold plasmas and perpendicular (Adlam and Allen 1958; Davis, Lüst and Schlüter 1958), parallel (Saffman 1961a), and oblique (Saffman 1961b; Kellogg 1964; Cordey and Saffman 1967) propagation and more recently for warm plasmas (Inoue 1968, 1969; Crevier and Tidman 1970). The qualitative description of nonlinear waves agrees with the properties deduced from the linear waves although there are some quantitative differences. In general the nonlinear wave appears as a pulse of magnetic field (large amplitude) traveling at a velocity faster than the fast wave speed and either preceded by or followed by a wave train. These nonlinear wave trains have relevance for collisionless shocks since a small amount of dissipation will damp the wave trains (leading or preceding) and a transition from state one to state two as indicated in Fig. 1 will have been achieved (Sagdeev 1962a, 1966).

As in the case of linear waves there is a small angle ϕ of order ϵ (for $M_A \ll \epsilon^{-1}$) which separates the leading from trailing wave trains. The characteristic length for nonlinear waves propagating perpendicular to the magnetic field is of order R_e while for oblique propagation the scale length is of order R_i which is considerably broader. There is an upper limit to the Alfvén Mach number above which nonlinear solutions to the two fluid equations have not been found. The significance of this limit will be discussed in Section II-C.

B. Dissipation

For large Alfvén Mach numbers, dissipation increases. If there is enough dissipation, the oscillations in the wave train will be either critically or over-damped resulting in a monotonic shock structure. Dissipation results from plasma turbulence which is generated by unstable plasma waves. The unstable waves must eventually return their energy to the

particles, and this process can proceed by several routes, e. g. resonant damping directly into particles and mode-mode coupling into waves which are then damped into particles. Due to the complexity arising from the large number of possible plasma waves, theorists have attempted to explain collisionless dissipation in terms of particular instabilities and many have been suggested. We will discuss only those which relate to direct observations.

For perpendicular shocks, large gradients in magnetic field are possible due to the small scale of the collisionless length R_e . It was recognized early (Sagdeev 1962a, 1962b; Kellogg 1964) that the electron current flowing in the plane of the shock perpendicular to \underline{B} and creating the jump in \underline{B} would produce unstable electrostatic plasma waves. If the relative streaming velocity between ions and electrons, V_d , is greater than the electron thermal velocity ($V_d > C_e$), a strong two-stream instability can create enough plasma turbulence to provide a "collisionless" resistivity and preferentially heat electrons (Buneman 1959). The primary effect of this instability is to limit the streaming velocity to the order of the electron thermal velocity. Sagdeev (1962a, 1966) pointed out that for a low β , low Mach number, perpendicular shock, this limitation on V_d due to plasma turbulence increases the leading gradient length to be of order $R_e \beta^{-\frac{1}{2}}$. This observation is an example of how dissipation can replace dispersion in determining gradient lengths.

A weaker current than that required to excite the two-stream instability can also produce unstable, electrostatic, plasma wave turbulence if the electron temperature exceeds the ion temperature. An analysis using a kinetic description (Jackson 1960; Stringer 1964) shows that when $T_e > 5 - 10 T_i$, a relative drift between ions and electrons in excess of the ion acoustic speed $C_S > KT/m_i$ causes the ion acoustic wave mode to be unstable. This instability involves ion plasma oscillations and frequencies up to ω_{pi} . In contrast to the two-stream instability which limits the flow velocity of electrons, this weaker ion acoustic instability gives rise to stochastic electric fields E_k which produce an effective resistivity for electrons with the result that their random velocity and thus their temperature is increased. The collisionless resistive dissipation produced by this mode of plasma turbulence has received the most theoretical attention.

A rough estimate can be made of the maximum amount of heating which can occur as a result of stochastic encounters with turbulent electric fields E_k . In a single encounter the maximum change in velocity, ΔV_s , a particle can acquire by interacting with a coherent wave packet is $\Delta V_s = eE_k/m\omega_d$ where $\omega_d = \omega - kV$ is the effective wave frequency as seen by a particle traveling with velocity V . In a succession of stochastic encounters, the particle random walks in velocity space with the total ΔV increasing as the square root of the number of encounters. If a particle spends a time t_0 in the turbulent field, the total number of random changes ΔV_s is t_0/τ where τ is the wave packet coherence time. An estimate for the temperature increase is thus given by

$$K \Delta T \sim \frac{1}{2} m (\Delta V)^2 \sim \frac{e^2}{2m\omega_d^2} E_k^2 \frac{t_o}{\tau} \quad (2)$$

The thermal energy density produced can be expressed in terms of the energy density contained in the electric field oscillations $W_k = \epsilon_o E_k^2/2$;

$$nK \Delta T \sim \frac{\omega_p^2}{\omega_d^2} \frac{t_o}{\tau} W_k \quad (3)$$

Equations (2) and (3) are general and not specific to the type of particle or type of turbulence. Estimates of this type can be used for comparison with observations of turbulence.

More detailed calculations have been carried out by a number of authors. The early work on ion acoustic wave turbulence neglected the presence of the ambient magnetic field. Kadomtsev (1965) has calculated that a large amplitude of turbulent fluctuations with a wave number spectral density which varies as $k^{-3} \ln(k\lambda_D)^{-1}$ would result from balancing the production of waves by linear growth against nonlinear wave scattering by the ions. Sagdeev (1967) has calculated on the basis of a quasilinear theory that this microturbulence could produce an effective collision frequency for electrons of $\nu_e \sim 10^{-2} (T_e V_d/T_i C_S) \omega_{pi} \sim 0.1 - 1 \omega_{pi}$ which is several orders of magnitude larger than would be expected on the basis of coulomb collisions. Krall and Book (1969a, 1969b) have extended the calculation of Sagdeev by including the effect of the magnetic field. By means of a quasilinear theory they arrive at an estimate for the shock thickness $L_S = (3R_e/2) \ln \frac{\omega_{pe}}{\omega_{ce}}$ which seems to agree well with several experiments in which the ratio ω_{pe}/ω_{ce} ranges over more than an order of magnitude. This theory has recently been refined (Biskamp 1970). Bekshtein and Sagdeev (1970) have reconsidered the wave damping by ions and arrive at a different scaling for the shock thickness, $L_S \sim (m_i/m_e)^4 R_e$, which is also consistent with observations.

We now turn our attention to two theoretical suggestions for ion dissipation mechanisms which apply primarily to perpendicular and oblique shocks respectively. The first (Tidman 1967a) involves an electrostatic ion-ion two-stream instability whose main result is to heat the upstream ions by interacting directly with the downstream ions traveling at a smaller velocity. A simple criterion for this instability to be operative is $\Delta V_i < C_S$ where ΔV_i is the relative drift between the cold upstream and hot downstream ions. It is difficult to estimate the amount of ion heating produced since the conditions necessary for this instability, hot electrons and low

relative ion drift, are not easily met; a recent calculation (Forslund and Shonk 1970) indicates that two interpenetrating ion streams do not thermalize effectively by this mechanism.

The second form of ion dissipation is associated with electromagnetic wave turbulence. This turbulence is produced by the fast mode (see Fig. 2) propagating obliquely to the magnetic field and above the ion gyrofrequency, the so-called whistler wave (Storey 1953). An early collisionless shock theory (Fishman, Kantrowitz and Petschek 1960; Camac et al. 1962) suggested that the whistler waves which had group velocities equal to the upstream flow would remain in the vicinity of the shock a long time and be greatly amplified. This theory assumed no damping of the waves and hence the upstream flow energy was dissipated into magnetic field turbulence. This assumption has been found to be invalid as the measured amplitude of the wave turbulence is too small to account for the dissipation (Patrick and Pugh 1969). Instead, the latter authors estimate that these waves provide the required dissipation by direct scattering of the ions by the wave electric fields according to the scheme leading to Eq. (2). Although this suggestion is plausible, no detailed calculation of the amount of ion heating by this mechanism has been performed.

C. Critical Mach Number

We have already mentioned that at a sufficiently large Mach number, low β , perpendicular shocks undergo a transition from an oscillatory to a monotonic structure due to increased turbulence. At a higher Mach number experimentally determined to be around $2.5 < M_A < 3.0$, a perpendicular, low β shock undergoes another change in structure which will be described later. The ion acoustic turbulence which has been described previously results in an effective resistivity and preferentially heats electrons. It has been widely suggested that the observed change in structure is related to the fact that there is a maximum Mach number for which resistivity alone can provide the required dissipation. This phenomenon is analogous to the situation in ordinary gasdynamics where there is a critical Mach number above which a shock with a continuous structure cannot be formed in a gas of zero viscosity but finite thermal conductivity (Landau and Lifshitz 1959). In a plasma in which the ions do not undergo any classical collisions, some kind of anomalous ion viscosity is required to achieve higher Mach number shocks.

The two fluid equations with no dissipation permit no solution when the flow velocity through a large amplitude structure is decreased to the ion acoustic speed C_S . For a cold plasma ($C_S = 0$) and perpendicular propagation, the ion flow velocity is reduced to zero at $M_A = 2$ (Adlam and Allen 1958; Davis et al. 1958). For high Mach numbers, a significant fraction of the ion stream would be reflected forward and the assumption of a single ion stream is violated. This phenomenon is called "wave breaking" but has not been observed in the laboratory. Instead, for Mach numbers this large, there is always sufficient dissipation that a monotonic structure does form with downstream properties specified by the Rankine-Hugoniot conditions.

The critical Mach number, M^* , above which a shock without ion viscosity cannot be formed is given by the condition that the downstream flow velocity equals the downstream ion acoustic speed, $V_2 = C_{S2}$. Woods (1969a) and Coffey (1970) have discussed the value of the critical Mach number for perpendicular shocks and find that for $\gamma = 5/3$, $M^* = 2.76$. Coroniti (1970) has discussed a possible explanation of why the critical downstream flow velocity is C_S which is a different velocity than the fast wave speed in a collisionless plasma. He showed that in a plasma with resistivity η , the fast wave speed decreases to C_S for scale lengths small compared to $L_M = \eta/\mu_0 V_2$, i. e., the magnetic field becomes decoupled from the plasma oscillations for a magnetic Reynolds number of order one. As a result, if $M_A < M^*$, a pulse from the piston traveling at the downstream fast wave speed approaches the shock from behind until it steepens enough to reduce its speed to C_{S2} which is less than V_2 and hence energy from the piston is blown downstream. However, for $M_A > M^*$, a pulse propagating toward the shock is slowed to C_{S2} which now exceeds V_2 . In this case the piston can feed additional energy to the shock, more energy than the shock can dissipate by resistivity alone.

It has been hypothesized that above the critical Mach number a viscous subshock forms (Marshall 1955; Kantrowitz and Petschek 1966; Coroniti 1970) in order to dissipate the additional energy. It was suggested that this subshock should have a smaller scale length over which viscous dissipation occurs, and this dissipation should interact directly with the ions allowing the formation of higher Mach number shocks. Indeed numerical integration of the two fluid equations including ion viscosity introduced artificially indicates that the shock structure can separate into a thin layer where viscous ion heating takes place imbedded within a broader magnetic structure (Macmahon 1968). Regardless of the details of the viscous dissipation region a broad structure is expected due to the gyration of the heated ions in the magnetic field. Woods (1969b) has carried out a detailed analysis based on ion orbits and found that the observed width is of order R_i which is identical to an ion gyroradius based upon the Alfvén speed ($R_i \equiv C_A/\omega_{ci}$).

The suggestion of the formation of a viscous subshock is based upon a thickest shock hypothesis. This hypothesis states that the dominant dissipation mechanism is the one which operates on the smallest gradient and can provide the required dissipation (Kantrowitz and Petschek 1966). In a collisionless plasma there is no a priori reason why at higher Mach number a viscous "subshock" should form because the viscous dissipation could have a larger scale length than that associated with resistivity. At low Mach number this viscous dissipation may not be operative due to its instability threshold level and hence the thickest shock hypothesis may still be valid. For perpendicular shocks, there is no definite observation of the scale length, broad or thin, of the dissipation mechanism which produces ion heating. There has been a theoretical suggestion (Tidman 1967b) that the ion heating may take place in a thin layer of order several $\lambda_D = C_e/\omega_{pe}$ at the rear of the magnetic shock structure. This heating is due to electrostatic turbulence resulting from an ion-ion streaming instability discussed in Section II-B.

III. EXPERIMENTAL TECHNIQUES

A number of experimenters have built devices to produce and study collision-free shock waves and they have met with varying degrees of success. Among the problem areas most usually encountered are: (1) failure to attain collision-free conditions ahead, within, and behind the shock; (2) not enough time or space for a shock to detach from the piston and achieve a steady structure; (3) insufficient spatial or temporal probe resolution to study shock structure; and (4) density gradients in the flow and finite radius of curvature effects which render the shock nonplanar.

These effects as well as the following considerations define regions in parameter space within which one can do collision-free shock experiments. An upper limit to the upstream plasma density is set by the collisional mean free path. The mean free path for coulomb collisions between ions in the upstream flow and those in the shock must be larger than the shock thickness. Since this mean free path scales as the square of the ion kinetic energy, upstream velocities greater than 10^7 cm/sec yield mean free paths greater than 0.25 meters even for relatively high densities equal to $10^{15}/\text{cm}^3$.

It is also necessary to have the classical conductivity due to electron collisions large enough so that the transverse current which creates changes in the magnetic field cannot produce significant dissipation (joule heating). The most restrictive requirement is that the electron mean free path in the upstream plasma be sufficiently long so that the turbulence is not damped by classical collisions. The electron temperature ahead of the shock must be greater than 1 eV to prevent such damping for laboratory experiments with upstream densities in excess of $10^{14}/\text{cm}^3$.

A lower limit on the upstream density is fixed by requiring that the shock thickness be small compared to the size of the device while the largest characteristic dimension in the plasma, $R_i = c/\omega_{pi}$, be small compared to the flow dimension. The length, R_i , is inversely proportional to the square root of the plasma density and is approximately 3 cm when the plasma density is $10^{14}/\text{cm}^3$. Hence, to obtain a relevant collisionless plasma shock experiment, the velocity and density must both be large. This requirement leads to a power level at least of the order of 10^7 watts for either a pulsed or steady experiment.

The maximum value of upstream magnetic field is limited by the requirement that the upstream flow velocity be at least equal to the Alfvén speed, i. e. $M_A \geq 1$. To date, workers have achieved maximum flow velocities of the order 5×10^7 cm/sec which limits the maximum magnetic field to a few kilogauss for densities of the order $10^{14}/\text{cm}^3$. The lower limit on the magnetic field comes from requiring that the largest possible

scale length, the ion gyro radius, be less than the size of the device. Approximately 50 gauss is the lower limit for velocities of 5×10^7 cm/sec and 0.5 meter scale size experiments.

There are many compromises that must be made in the choice of parameters for a given experiment and to date no single experiment satisfies all the requirements for any appreciable range of M_A and β . Shock experiments can be divided into two categories: steady and unsteady. In the former, a super-Alfvénic plasma is blown against an obstacle producing a standing shock in much the same manner as a wind tunnel. In the latter, a piston is accelerated to super Alfvénic velocity into a stationary plasma producing a shock running out ahead as in an ordinary shock tube. The piston may take on various forms, including rapidly moving electric and magnetic field gradients or a slug of high density plasma.

A plasma wind tunnel was built by Patrick and Pugh (1967, 1969) in which a fully ionized plasma was blown against a magnetic dipole cavity producing a standing oblique shock wave analogous to the Earth's bow shock as shown in Fig. 4a. The upstream plasma electron temperature and density were approximately 10 eV and $5 \times 10^{13}/\text{cm}^3$ corresponding to an upstream mean free path of 30 cm which is comparable to the scale size of the experiment. Thus, the high T_e upstream makes this experiment truly collision-free on both sides of the shock. The shock thickness, $\sim 3 R_i \approx 10$ cm, is large enough to resolve shock structure, but it is possible that two dimensional effects caused by density gradients in the flow and a finite radius of curvature of the shock may be important. The minimum upstream B is limited by residual fields from the plasma source limiting the maximum Mach number and β to be below three and one, respectively. The Rankine-Hugoniot jump conditions have been verified and detailed spatial turbulence measurements have been obtained. Self-consistency is achieved: the measured turbulence provides sufficient dissipation to satisfy the jump conditions.

Unsteady shocks have also been produced by rapidly imploding magnetic field gradients in devices called Z and θ pinches. In Fig. 4b we show a schematic diagram of a Z pinch (Paul et al. 1965). The initial plasma is produced by an oscillatory axial current which first ionizes then heats the background gas to densities and temperatures of approximately $7 \times 10^{14}/\text{cm}^3$ and 1 eV, respectively, giving an electron-ion mean free path in the upstream plasma of order 0.5 mm. Thus, the plasma is collisional. The shock is produced by a rapid rise in axial current which causes the azimuthal magnetic field to implode, driving a cylindrically converging perpendicular shock into the initial plasma. Shock speeds up to 25 cm/ μ sec have been achieved with Mach numbers in the range $2 \lesssim M_A \lesssim 6$. The shocks are thin ($L_S \lesssim 1$ cm) compared to flow dimensions and detach from the piston to become steady for about 10 cm before convergence effects arise. For low Mach number perpendicular shocks, precursor waves cannot propagate and thus the fact that the upstream plasma is collisional may not be of great significance. These experiments at low M_A are also self-consistent in that measured turbulence levels (Paul, Daughney and Holmes 1969) can account for the required dissipation. For larger M_A , the shock thickens and, since the

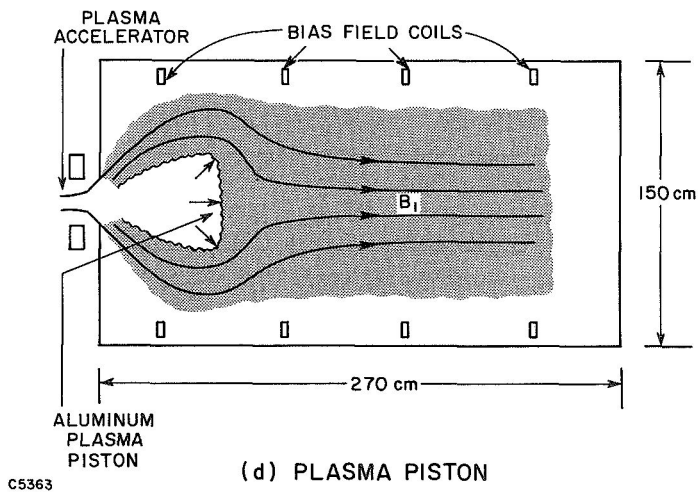
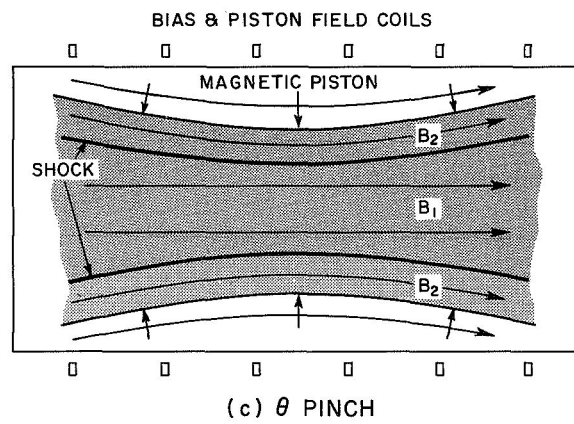
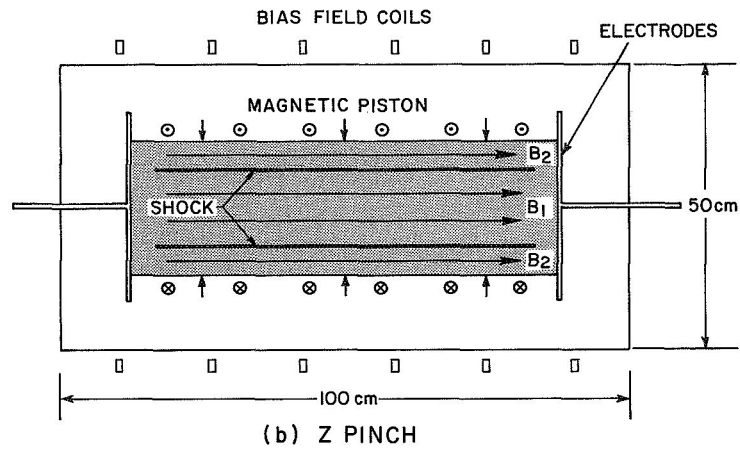


Fig. 4 Schematic Diagrams of Laboratory Experiments

upstream conductivity is low, the shock structure can be affected by collisional damping. Also, for these higher values of M_A , the shock thickness becomes comparable to the scale size of the experiment.

Another version of this imploding shock device is the θ pinch shown schematically in Fig. 4c and built by many experimenters (Alikhanov et al. 1969; Chodura et al. 1969; Hintz 1969; DeSilva et al. 1969; Zagorodnikov, Smolkin and Sholin 1967). These perpendicular shocks are produced by a rapidly imploding axial field driven by an azimuthal current as opposed to the axial current of the Z pinch. The upstream plasma is produced by either electric discharges or photoionization. In the Z pinch, the piston field is perpendicular to the bias field while for θ pinch experiments the B fields are either parallel or antiparallel.

The results from these numerous θ pinch experiments span a wide range of parameters. For upstream densities below $10^{13}/\text{cm}^3$, steady, detached shocks are not observed (Chodura et al. 1969; DeSilva et al. 1969) while for densities of the order of $10^{14}/\text{cm}^3$ the results of Paul et al. (1965) are recovered. For high β and Mach number, i. e. $\beta \gtrsim 1$ and $M_A \gtrsim 4$ (Hintz 1969; Chodura et al. 1969), shocks are observed but are considerably thicker (or order $R_i \approx 1$ cm) than the low β , low M_A case. It is important to note that many of the results of the θ pinch experiments are characteristic of the specific device and may not be associated with collisionless shock waves themselves; e. g. , DeSilva et al. (1969) find no clear shock structure for antiparallel piston and bias fields while Hintz (1969) observes a more pronounced shock structure for the antiparallel case.

An interesting variation of the perpendicular θ pinch is that built by Robson and Sheffield (1969) in which a short θ pinch coil is used and a curved piston with oblique propagation is produced. The upstream plasma is collisional and a large amplitude damped whistler wave is observed out ahead of a sharp rise in the magnetic field, the width of the total structure approaching $R_i \sim 1$ cm. No turbulence is observed and it is unclear if any collisionless dissipation mechanisms are involved except close to the centerline where the shock is perpendicular and the results of Paul et al. (1965) are again recovered.

Another unsteady experiment is shown in Fig. 4d which produces an oblique disturbance (Friedman and Patrick 1968, 1970). Here a coaxial gun ionizes and accelerates a mass of aluminum wire and injects it into a background, magnetized plasma at 10^7 cm/sec. Preionization is achieved by ultraviolet radiation from the gun. The upstream density is approximately $10^{15}/\text{cm}^3$ and thus, for an estimated electron temperature between 1 and 10 eV, the upstream plasma is highly collisional ($\lambda \approx 1$ mm). Alfvén Mach numbers range from 30 up to several hundred and the upstream β is order 1 - 10. It is not clear whether or not a shock forms; however, a momentum transfer mechanism on a scale less than 1 cm, which is of the order of R_i , is present for $M_A \lesssim 100$. At higher M_A , little coupling is observed.

IV. COMPARISON OF EXPERIMENT AND THEORY

For perpendicular propagation and low β , the character of the shock structure changes significantly as the Mach number is increased from unity. In Section IV A we first discuss this sequence and then discuss high β shocks. In Section IV B we present the experimental results for oblique shocks. We shall compare experimental results with the theoretical work discussed in Section II.

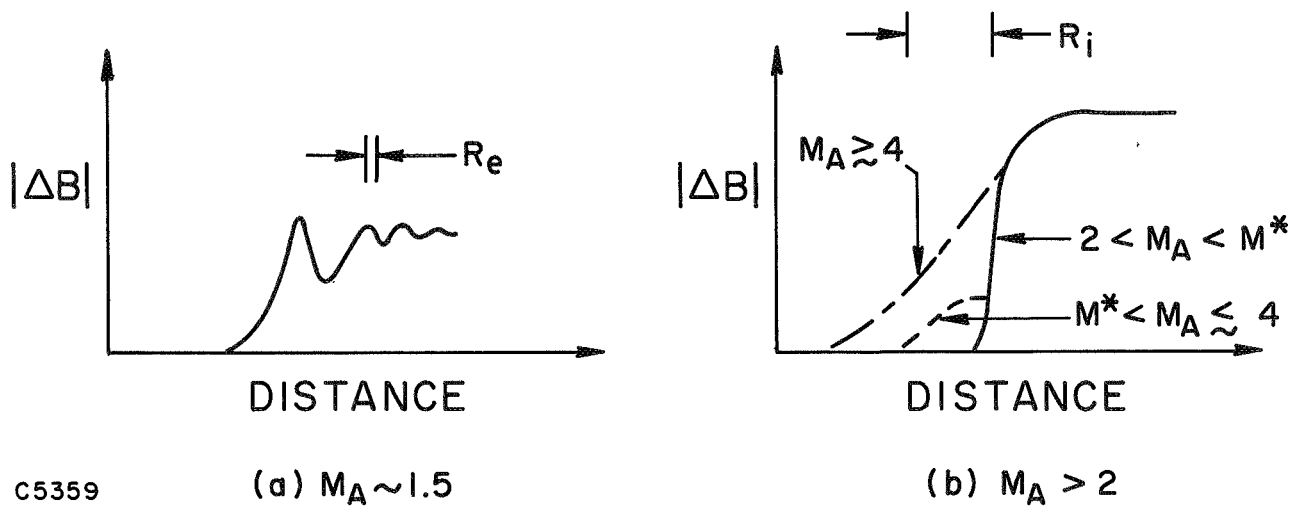
A. Perpendicular Shocks

$1 < M_A < 2$, low β . - In this Mach number range, the shock structure is dominated by dispersion rather than dissipation resulting in the shock structure shown schematically in Fig. 5a. (Hintz 1969; Alikhanov et al. 1969). The initial gradient length is of order $R_e = c/\omega_{pe}$ followed by a damped wave train of wavelength $\sim 10 R_e$. These observations agree with the earlier theoretical discussion in that both linear and non-linear wave theories predict for these conditions initial gradient lengths of order R_e followed by a trailing wave train with wavelength of the order a few times R_e .

Although dissipation is not dominant it is manifest in the damping of the wave train. Since for these low β experiments, $10^{-2} < \beta < 10^{-1}$, a Mach number of 1.5 exceeds the two stream instability threshold (Sagdeev 1962a, 1966), the initial shock gradient should be given by $L_S \sim R_e \beta^{-1/2} = 3 - 10 R_e$ as discussed in Section II B. No direct evidence exists at this time to distinguish collisional from turbulent dissipation.

$2 < M_A < M^*$, low β . - At higher Alfvén Mach numbers, dissipation is strong enough to completely damp out the trailing wave train and shock structures become monotonic with thicknesses of the order $10 R_e$ as shown in Fig. 5b. (Alikhanov et al. 1969; Hintz 1969; Paul et al. 1965; Goldenbaum 1967). The electron temperature jump across the shock has been measured by the Thompson scattering of laser light (Paul et al. 1967; DeSilva and Stamper 1967; Chodura et al. 1969) and the results show that the rise in T_e alone is sufficient to account for the increase in β required by the Rankine-Hugoniot conditions. It is concluded therefore that only the electrons are heated (by joule dissipation) and that no ion heating or viscosity is present.

The shock width is larger than would be expected if no electron collisions were present and it is concluded that an anomalous resistivity exists which has broadened the shock front beyond the collisionless skin depth R_e . An estimate of the amount of resistivity or equivalently, the effective collision frequency, ν_e , is obtained by assuming the shock has a magnetic Reynolds number R_m , of the order of unity,



C5359

(a) $M_A \sim 1.5$

(b) $M_A > 2$

Fig. 5 Typical Perpendicular Shock Structures for $\beta \ll 1$ and
 (a) $M_A \sim 1.5$, (b) $M_A > 2$

$$R_m = \mu_o \sigma L_S V_1 \approx 1$$

where

$$\sigma = e^2 n (m_e v_e)^{-1}; \quad L_S \sim 10 R_e$$

For $n = 7 \times 10^{14}/\text{cm}^3$ and $V_1 = 2.4 \times 10^7$ cm/sec (Paul et al. 1965), the effective collision frequency is of the order ω_{pi} . This value exceeds the classical value (Spitzer and Härm 1953) based upon coulomb collisions for measured electron temperatures in the shock front by at least two orders of magnitude. Frequencies of this order have been detected by probes (Alikhanov et al. 1969) and by laser scattering (Paul, Daughney and Holmes 1969). The latter authors have measured enhanced laser scattering from coherent density fluctuations to be between two and three orders of magnitude greater than that expected from random fluctuations. Their calculations show that this turbulence gives rise to an anomalous resistivity which can provide the required dissipation.

For Alfvén Mach numbers in the range, $2 < M_A < M^*$, the electron drift velocity associated with the transverse current exceeds C_S and if $T_e \ll T_i$ in the upstream plasma, the current is unstable as discussed in Section II B. Even in the one experiment where $T_e < T_i$ (Chodura et al. 1969), it is thought that some other mechanism, possibly the two stream instability preheats the electrons until T_e becomes greater than T_i in the shock front and then the current is unstable. The frequencies observed are of the order ω_{pi} in agreement with theory; furthermore, the turbulent wave number spectrum predicted by Kadomtsev (1965) has been experimentally verified by Daughney, Holmes and Paul (1970). We also mention again that Krall and Book's (1969b) theory yields a shock thickness

$$L_S = \frac{3}{2} R_e \ln \frac{\omega_{pe}}{\omega_{ce}}$$

which agrees well with several experiments in which the ratio ω_{pe}/ω_{ce} ranges over more than an order of magnitude.

The conclusions to be reached for $2 < M_A < M^*$ are: (a) The scale length of the shock thickness is of order $10 R_e$; (b) Perpendicular shocks are resistive with the primary dissipation mechanism being joule dissipation; (c) Theory and experiment appear to be in substantial agreement that ion acoustic wave turbulence produces the required anomalously large resistivity.

$M^* < M_A < 4$, low β . - As the Mach number is increased beyond a critical value experimentally determined to be about 2.7, the character of

the shock changes as indicated schematically in Fig. 5b. The shock grows a broad foot at the leading edge while at the rear the steep gradients present at lower Mach numbers are still observed (Paul et al. 1965; Alikhanov et al. 1969; Hintz 1969). Measurements of the ion velocity distribution now show an effective ion thermalization (Alinovskii et al. 1970) whereas for $M_A < M^*$ no ion heating was observed. The scale length of the broad foot is of order R_i as to be expected when hot ions are present (Woods 1969b). No detailed turbulence measurements have been made on the broad foot portion of these shocks but the fluctuation level detected by laser scattering does not appear to be as great as that associated with the steep gradient shocks at lower Mach number (Paul, Daughney and Holmes 1969). The presence of thermalized ions violates the single streaming hypothesis of the two fluid description and either a full kinetic theory or a multi-ion fluid description is necessary.

The appearance of the broad foot is related to the fact that these Mach numbers exceed the critical Mach number discussed in the theoretical section and therefore joule heating is insufficient to provide the required dissipation. The ions must acquire some randomization in velocity producing counter streaming ions in the broad foot. This configuration may be unstable (Sagdeev 1966) leading to fluctuations with frequencies of the order $(\omega_{ce}\omega_{ci})^{1/2}$ for which there is some laboratory evidence (Zagorodnikov et al. 1967). However, the mechanism leading to ion viscosity and producing ion heating is still unclear. Tidman's (1967b) suggestion of a thin subshock has not been verified; the spatial resolution of shock experiments is not great enough to either confirm or deny even the existence of a thin subshock. A theory based upon the orbiting motion of ions reflected from the shock by the electrostatic potential and hot ions diffusing upstream (Woods 1969b) is in agreement with observations (Paul 1965); however, it must be emphasized that the upstream plasma is collisional and thus the measured scale lengths may not be totally determined by collisionless processes.

$4 < M_A$, low β . - For the low β , high Mach number case, the total shock structure thickens to R_i and the double structure disappears as shown in Fig. 5b. (Paul et al. 1965; Hintz 1969; Chodura et al. 1969). Perpendicular shocks at low β have not been produced much beyond $M_A \approx 6$.

High β . - For moderate $\beta \approx 1$ and low $M_A < M^*$, the shock is similar to the low β case (Hintz 1969) with $L_S \sim 10 R_e$. Above the critical Mach number the shock thickens as a whole and no double structure is observed. At high M_A , the shock thickness approaches R_i .

For high β of order 5 and moderate Mach number of order 4, the shock is thicker than the low β case, of order R_i (Chodura 1969). Significant ion heating is observed both above and below the critical Mach number and ion heating generally increases with increasing Mach number. However, since these are thicker shocks and the upstream plasma is collisional, the collisionless turbulent processes may be altered.

B. Oblique Shocks

When the shock is not perpendicular to \underline{B} , collisionless shock structure changes significantly and precursor wave trains with shock thicknesses of the order R_i are expected. Waves of this type have been observed (Patrick and Pugh 1967, Robson and Sheffield 1969) although significant differences exist between these two experiments. Patrick and Pugh (1967) see a standing shock produced by the interaction of a super Alfvénic flow and a magnetic dipole in a simulation experiment of the Earth's bow shock. The shock thickness is of order a few R_i for Mach numbers in the range $1.5 \lesssim M_A \lesssim 3$ and the Rankine-Hugoniot jump conditions are obeyed. A broad spectrum of turbulent whistler waves with frequencies up to a few times ω_{ci} is observed ahead of the shock. The upstream plasma is collisionless and there is ample time for transients to decay and turbulence to develop. The turbulence level is not large enough to account for the dissipation purely in terms of wave energy in contrast to the early theory of Camac et al. (1962), however, an estimate of ion thermalization due to ion scattering off the waves (Patrick and Pugh 1969) as obtained from Eq. (2) in Section II B may be sufficient to account for the required dissipation. It is to be noted (Patrick and Pugh 1969) that when one compares the laboratory turbulence data with Earth bow shock data, the turbulence levels are quite similar indicating that whistler wave turbulence is an important feature of oblique collisionless shocks, both in the laboratory and space as discussed in the next section.

A moving oblique shock has been generated from a curved magnetic piston in a modified θ pinch apparatus (Robson and Sheffield 1969). A single damped whistler wave train out ahead of a magnetic field compression is observed with overall structure of the order R_i . The upstream plasma is collisional and it is not clear that turbulence has had a chance to develop. The dispersion characteristics and magnetic field polarizations of the wave train have been measured and these observations agree well with the concept of a whistler with sufficient group velocity to stand in the upstream flow.

A disturbance propagating obliquely to the magnetic field at very high number Mach number ($30 < M_A < 10^3$) has been produced by injecting a highly ionized aluminum plasma at speeds of order 10^7 cm/sec into a weakly magnetized plasma (Friedman and Patrick 1968). The low Alfvén velocity C_A is achieved by totally ionizing the background gas with the ultraviolet pulse from the accelerator discharge. Since the piston is constantly decelerating, and the upstream plasma is collisional, it is not certain that a shock has formed. The main result of this experiment is that the momentum coupling of the piston with the background plasma depends on the value of ambient magnetic field. With no magnetic field applied, the two plasmas interpenetrate freely with little coupling. When a weak magnetic field is applied upstream, the aluminum plasma decelerates rapidly effectively exchanging its momentum with all the background plasma which it encounters. This magnetic field is too small to provide a significant magnetic pressure or to affect the motion of the aluminum ions. The nature of the momentum transfer mechanism is not understood.

Interferometric measurements indicate that the aluminum plasma-background plasma interface is no thicker than the resolution capability of the diagnostic which is of order $R_i \sim 0.5$ cm (Friedman and Patrick 1970). The Mach number below which coupling seems to take place is around one hundred. The turbulence spectrum of the magnetic field or density fluctuations has not been completely measured to date. However, laser scattering experiments indicate a large level of plasma density fluctuations is present. ✓

V. EARTH'S BOW SHOCK

The solar corona expands forming a radially outward flow of particles, predominantly fully ionized hydrogen, which has been called the solar wind. The solar wind was first predicted (Parker 1958) and later confirmed by direct measurement (Neugebauer and Snyder 1962) to have a flow velocity in excess of the Alfvén speed in the vicinity of the Earth. The Earth's dipole magnetic field forms an impenetrable body for scale sizes larger than an ion gyroradius ($\sim 10^2$ km) and a shock has been observed (Ness et al. 1964) to stand in the flow ahead of the Earth.

A schematic diagram of the interaction of the solar wind with the Earth's dipole magnetic field in the ecliptic plane is shown in Fig. 6. The properties of the upstream solar wind vary widely due to solar activity, but typical values are indicated in Fig. 6; under unusual conditions actual values can differ by more than an order of magnitude from those quoted. The collision mean free path is of order the distance from the Earth to the sun and hence the structure of the flow by the Earth is truly collisionless. The angle between the magnetic field direction and the flow direction is 45° on the average, but has a large variance. Because of the wide variation in the magnetic field direction the shock is generally oblique.

The shock separates the relatively quiet interplanetary magnetic field from the more compressed and turbulent magnetic field in the magnetosheath. The shape of the shock surface, the Mach angle and the standoff distance (Ness et al. 1964) are given very well by MHD fluid equations (Spreiter and Jones 1963; Spreiter, Summers and Alksne 1966; Spreiter and Alksne 1970). The justification for this fact is attributed to the presence of scale sizes such as the ion gyroradius ($\sim 10^2$ km) which are much smaller than the flow scale size ($\sim 10^5$ km). Typical values of the ion and electron inertial scale lengths are $R_i \sim 50 - 100$ km and $R_e \sim 1 - 2$ km. Hence all relevant collisionless scale lengths including the Debye length (~ 20 meters) are resolvable by satellite measurements.

An important feature of the Earth's bow shock is that it is constantly in motion; this fact complicates interpretation of data. Since data are taken in the satellite reference frame, scale lengths and frequencies appropriate to a particular physical process often depend upon the relative velocity between the satellite and the shock and/or particles. On many occasions (Holzer, McCleod and Smith 1966; Heppner et al. 1967) the shock appears to oscillate with maximum excursion of the order an Earth radius and an average shock velocity of approximately 10 km/sec. On other occasions (Fredericks et al. 1970) the shock motion is quite different and might be explained by a corrugation traveling along the shock surface.

$n \sim 3-10 \text{ cm}^{-3}$
 $|B| \sim 4-7 \gamma (1\gamma = 10^{-5} \text{ gauss})$
 $V \sim 300-700 \text{ km/sec}$
 $T_e \sim 10^5 \text{ }^\circ\text{K} \sim 10 \text{ eV}$
 $T_i \sim 2-10 \text{ eV}$
 $M_A \sim 5-10$
 $\beta \sim 0.3-3$
 $R_E = 6.4 \times 10^3 \text{ km}$

c5358

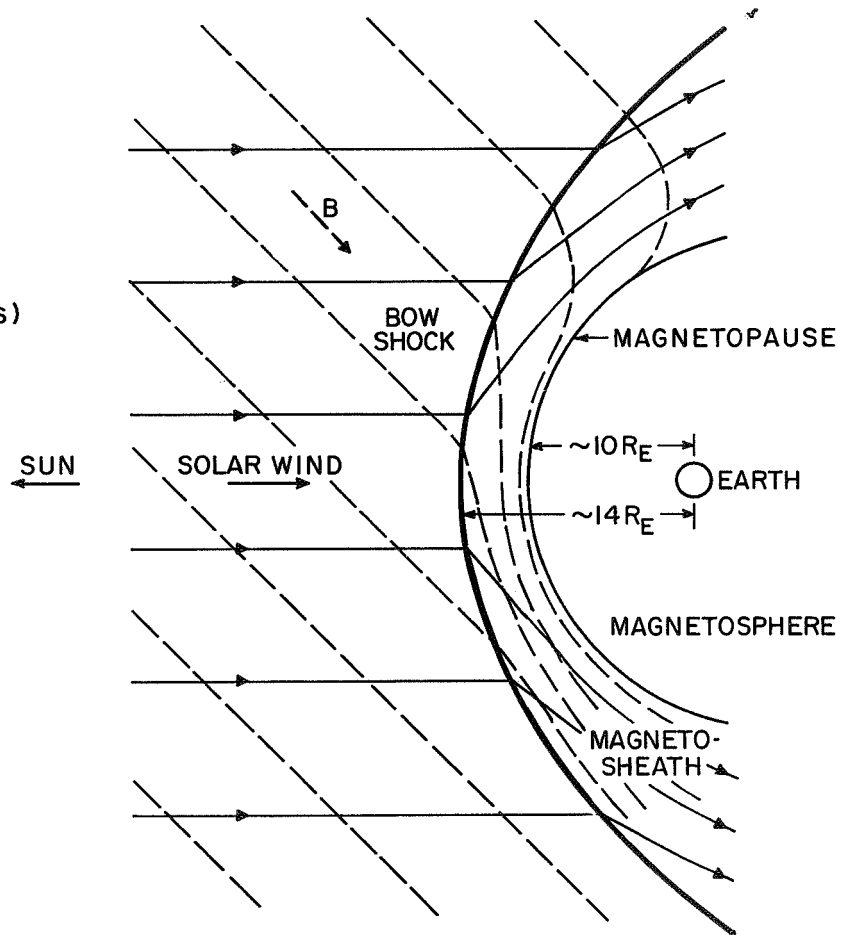


Fig. 6 Schematic Diagram of the Earth's Bow Shock

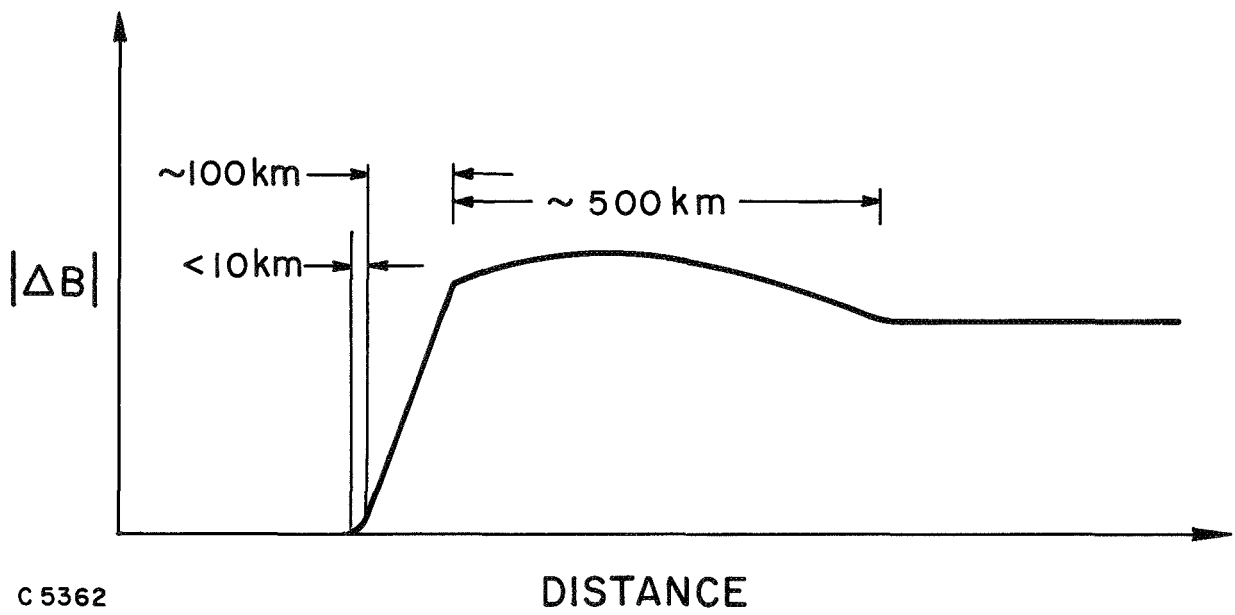
Since the typical shock velocity is in excess of the satellite velocity, of order 1 - 2 km/sec, meaningful data reduction requires knowledge of the shock velocity.

An average structure compiled from many observations (Ness et al. 1964, Heppner et al. 1967) taken with magnetometers having a low frequency cutoff of order 5 Hz is shown in Fig. 7. The initial B field gradient is observed to change within 1 - 2 seconds, the maximum compression is typically reached in about ten seconds, and the field relaxes in another 30 - 60 seconds. By assuming an average velocity of 10 km/sec, estimates for these scale lengths are as shown. The initial rise in B is of the order R_i and the full shock width is 5 - 10 R_i in agreement with laboratory simulations (Patrick and Pugh 1967) and the previous theoretical discussion of obliquely propagating waves.

The above description is an overall view of the shock structure; in actuality finer scale structure has been observed. A broad spectrum of whistler wave turbulence (Holzer et al. 1966; Smith et al. 1967; Russel, Olson and Holzer 1968; Olson, Holzer and Smith 1969) has been observed. The high turbulence level extends well into the shock structure since the magnetosheath is characterized by fluctuating magnetic fields. As one crosses the shock from the solar side, not only the amplitude of the turbulence increases but the shape of the spectra changes as well (Olson et al. 1969). Thus the increased amplitude (2-3 orders of magnitude increase in the power spectral density) cannot be explained as just a compression of the interplanetary field but indicates that waves are being generated in the shock. The shape of the spectra continues to change as one progresses into the magnetosheath. In general, above the ion gyrofrequency (~ 0.2 cps) the interplanetary spectrum falls off as (frequency) $^{-1}$ whereas in the shock and magnetosheath, the fall off is faster, roughly as (frequency) $^{-3}$.

The appropriately normalized spectrum of whistler wave turbulence measured in the bow shock has been compared to the spectrum measured in a laboratory simulation (Patrick and Pugh 1969). In Fig. 8 we show the power spectral density of the magnetic field oscillations multiplied by the frequency and normalized to the average value of magnetic field as a function of frequency normalized to the ion gyrofrequency. The spectrum is essentially flat below a few times the ion gyrofrequency. This observation is an indication that whistler waves with a group velocity sufficiently large to stand in the shock front are present. Although the turbulence level is insufficient to provide the dissipation on the basis of wave energy as in the theory of Camac et al. (1962), ion scattering may account for much of the turbulence as discussed in the theoretical section. The recent higher frequency data from OGO-III (Olson et al. 1969) indicate a higher level of turbulence and this discrepancy is not understood.

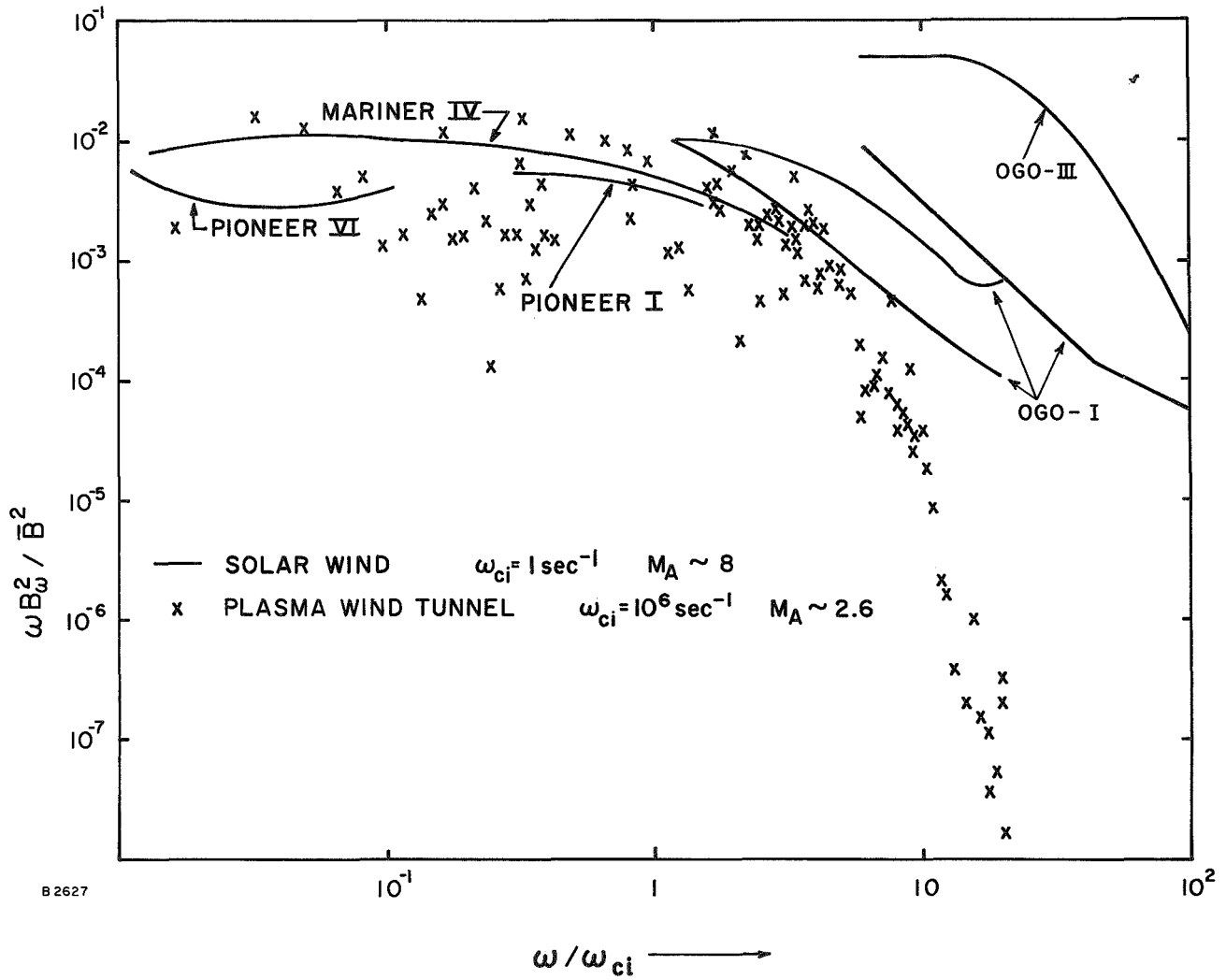
At higher Mach numbers, much higher frequency oscillations ($\sim 10^3$ Hz) have also been detected on occasion (Fredericks et al. 1968, 1970) which are electrostatic in nature, i. e., there are no corresponding



C 5362

DISTANCE

Fig. 7 Gross Magnetic Structure of the Bow Shock



B 2627

Fig. 8 Whistler Wave Turbulence Spectra Obtained in the Plasma Wind Tunnel (Patrick and Pugh 1969) and the Earth's Bow Shock

magnetic oscillations accompanying them. These bursts of electrostatic noise are associated with the steep gradients of the lower frequency whistler waves. The scale length of these gradients in B are observed to be as small as R_e suggesting that the electrostatic noise results from ion acoustic instabilities driven by transverse currents in much the same manner as observed in low Mach number perpendicular shocks.

The observations obtained thus far indicate a great variety of structures present in the bow shock. At a very low Mach number of $M_A = 1.5$ (Heppner et al. 1967), a smooth shock structure with little turbulence has been observed, while at higher Mach numbers ($M_A = 2-5$) whistler wave turbulence seems to dominate the shock structure. At very high Mach numbers, $M_A > 5$, both whistler wave and electrostatic wave turbulence may be present.

The subject of turbulence frequency spectra is somewhat obscured by the fact that none of the data has been Doppler shifted which requires a knowledge of both the phase velocity and the wave vector. For example, if the waves present in the shock front spectra are whistlers according to Camac et al. (1962), they must have a group velocity equal and opposite to the solar wind velocity which is of the order 400 km/sec. From the dispersion relation for these waves, their wavelength is several times R_i ($kR_i \sim 1$) or of the order 100 km. Thus, the Doppler shift, $\mathbf{k} \cdot \mathbf{V}$, is of the same order as the frequencies measured in the satellite frame. The Doppler shift can change the detailed shape of the spectra, but can neither shift the spectra to different frequency regimes nor fundamentally alter the physical conclusions. For the high frequency electrostatic waves, the Doppler shift will likewise be comparable to the measured frequencies. Detailed comparison of theory with the observations must wait until more information on this problem of Doppler shifting is available.

Another interesting feature of the shock is the observation of a flux of protons outward from the shock (Asbridge, Bame and Strong 1968). It appears that part of the solar wind is accelerated to higher velocities at the bow shock and then re-emitted forward. This forward reflection of ions is reminiscent of the existence of a critical Mach number for perpendicular laboratory shocks above which ion viscosity effects are important as discussed for perpendicular shocks.

In conclusion, the Earth's bow shock provides a laboratory for making detailed measurements of collisionless shock structure. The whistler wave turbulence seen at moderate Mach number for oblique shocks is similar to that observed in the laboratory. Measurements of the particle velocity distribution function are now becoming available which will allow an investigation of the ion thermalization process.

VI. SUMMARY

We have seen that shock waves exist in an ionized fluid flowing at super-Alfvenic speeds with a scale length much shorter than the collisional mean free path. A primary goal of collisionless shock research is to determine for what conditions shocks are thin and thus appear as a discontinuity in the fluid description of the flow. For low Mach number, low β , perpendicular shocks, the shocks are very thin, of the order $10 R_e$, whereas for all other conditions, i. e., higher Mach number, β , and/or oblique propagation, the shock is thicker, on the order of R_i . Since the ratio of R_i to R_e is just the square root of the mass ratio, the thicker shocks are only four times the thinner shocks for hydrogen. For moderate Mach number, the quantity R_i is comparable to the ion gyro radius (based upon flow velocity) since the ion gyro radius = $MA R_i$. Thus practically speaking, the thickness of collisionless shocks is always comparable to or less than the ion gyro radius. For flow scales which are large compared to the ion gyro radius, a fluid description is valid for the overall flow and the shock can be treated as a discontinuity in the collisionless fluid. Investigation of the shock structure on the other hand, requires a full kinetic description taking into account various turbulent dissipation mechanisms.

The dissipation which must be present in the shock structure in order to satisfy the Rankine-Hugoniot conditions arises from the interactions of the particles with turbulent waves which are generated and amplified in the shock. For low Mach numbers, dispersion effects determine the initial gradients in the shock while dissipation fixes the total shock thickness. At higher Mach numbers, dispersion is unimportant and dissipation alone determines the shock structure.

Three types of turbulent dissipation have been observed and progress has been made on understanding two of them. For perpendicular, low β shocks below the critical Mach number M^* , ion acoustic waves are driven unstable by transverse currents and the resulting turbulence scatters and heats electrons. This anomalous resistivity is sufficient to account for the required dissipation. At Mach numbers greater than M^* , ions are heated as a result of a viscous-like mechanism which is neither well documented nor well understood. For oblique shocks, a turbulent spectrum of whistler waves is observed in the shock front which appears to have a sufficient amplitude to scatter the ions an amount necessary to account for the required dissipation. Hence, for oblique and high Mach number perpendicular shocks, ions are heated directly in the shock.

More work is needed to obtain a better understanding of the structure of collisionless shocks. Laboratory experiments could provide detailed measurements of the turbulence which occurs in the shock front. Theoretical

work, which has been guided in the past by experimental observation, should progress to the point where critical tests of theoretical ideas can be suggested. As a result, experiments which explore the dependence of the shock thickness and structure on various parameters e. g., m_e/m_i and ω_{ce}/ω_{pe} , would be useful. As examples of more detailed comparisons of experiment and theory which should become more prevalent in the future we cite the comparison made by Daughney et al. (1970) with the predicted spectrum of Kadomtsev (1965), and the comparison of the theoretically predicted shock thickness made by Krall and Book (1969b) with the results obtained in several different experiments.

The most significant advance in the study of the Earth's bow shock will come from multiple satellite probes which allow the separation of spatial from temporal variations and the determination of the polarizations of the turbulent fields and wave vectors. Only then can meaningful measurements be made of the shock thickness and turbulent wavelengths so that Doppler shifts can be inferred.

The mechanism which leads to the anomalous ion viscosity in perpendicular shocks for Mach number greater than M^* still remains to be explained. In addition, more theoretical work is needed in order to explain the ion heating which occurs in oblique shocks due to whistler wave turbulence. At high Mach number ($M_A \sim 5 - 10$) the relative importance of (electromagnetic) whistler wave turbulence and fine scale (electrostatic) ion acoustic wave turbulence in providing dissipation needs to be critically assessed. Furthermore, the area of very high Alfvén Mach number where the energy contained in the magnetic field is insignificant as compared to kinetic energy is becoming more relevant as the possibility of forming electrostatic shocks, a topic not discussed in this review, is being actively investigated. The next few years should provide a considerable increase in our understanding of the above phenomena.

REFERENCES

- Adlam, J. H. , Allen, J. E. , Phil. Mag. , 3 , 448-455 (1958)
- Alikhanov, S. G. , et al. , Plasma Phys. and Contr. Nucl. Fus. Res. , 1 , 47-68 (IAEA, Vienna, 1969)
- Alinovskii, N. I. , Eselevich, V. G. , Koshilev, N. A. , Kurtmullaev, R. Kh. , Soviet Phys. JETP , 30 , 385-391 (1970)
- Asbridge, J. R. , Bame, S. J. , Strong, I. B. , J. Geophys. Res. , 73 , 5777-82 (1968)
- Axford, W. I. , J. Geophys. Res. , 67 , 3791-96 (1962)
- Bekshtein, G. E. , Sagdeev, R. Z. , JETP Lett. , 11 , 194-197 (1970)
- Biskamp, D. , J. Geophys. Res. , 75 , 4659-65 (1970)
- Bratenahl, A. , Yeates, C. M. , to be published Phys. Fluids (1970)
- Buneman, O. , Phys. Rev. , 115 , 503-517 (1959)
- Camac, M. , Kantrowitz, A. R. , Litvak, M. M. , Patrick, R. M. , Petschek, H. E. , Nuclear Fusion Supplement, Pt. 2 , 423-445 (1962)
- Chao, J. K. , J. Geophys. Res. , 75 , Nov. (1970)
- Chew, G. F. , Goldberger, M. L. , Low, F. E. , Proc. Roy. Soc. Lond. , A236 , 112-118 (1956)
- Chodura, R. , Keilhacker, M. , Kornherr, M. , Niedermeyer, H. , Plasma Phys. and Contr. Nucl. Fus. Res. , 1 , 81-92 (IAEA, Vienna, 1969)
- Coffey, T. P. , Phys. Fluids , 13 , 1249-58 (1970)
- Cordey, J. G. , Saffman, J. Plasma Phys. , 1 , 129-144 (1967)
- Coroniti, F. V. , J. Plasma Phys. , 4 , 265-282 (1970)
- Crevier, W. F. , Tidman, D. A. , Phys. Fluids , 13 , 2275-87 (1970)
- Daughney, C. C. , Holmes, L. S. , Paul, J. W. M. , Phys. Rev. Lett. , 25 , 497-499 (1970)

- Davis, L., Lüst, R., Schlüter, A., Z. Naturforsch., 13A, 916-936 (1958)
- DeSilva, A. W., et al., Plasma Phys. and Contr. Nucl. Fus. Res., 1, 143-153 (IAEA, Vienna, 1969)
- DeSilva, A. W., Stamper, J. A., Phys. Rev. Lett., 19, 1027-30 (1967)
- Fishman, F. J., Kantrowitz, A. R., Petschek, H. E., Rev. Mod. Phys., 32, 959-966 (1960)
- Formisano, V., Kennel, C. F., J. Plasma Phys., 3, 55-74 (1969)
- Forslund, D. W., Shonk, C. R., Phys. Rev. Lett., 25, 281-284 (1970)
- Fredericks, R. W., Kennel, C. F., Scarf, F. L., Crook, G. M., Green, I. M., Phys. Rev. Lett., 21, 1761-64 (1968)
- Fredericks, R. W., et al., J. Geophys. Res., 75, 3751-68 (1970)
- Friedman, H. W., Patrick, R. M., Bull. Am. Phys. Soc., 13, 1506 (1968)
- Friedman, H. W., Patrick, R. M., Avco Everett Research Report 355, to be submitted for publication in Phys. Fluids (1970)
- Gold, T., In Gas Dynamics of Cosmic Clouds, p. 103 (Burgers, J. M., Van de Hulst, J. C., Eds., North-Holland Publ. Co., Amsterdam, 260 pp., 1955)
- Goldenbaum, G. C., Phys. Fluids, 10, 1897-1904 (1967)
- Heppner, J. P., Sugiura, M., Skillman, T. L., Ledley, B. G., Campbell, M., J. Geophys. Res., 72, 5417-71 (1967)
- Hintz, E., Plasma Phys. and Contr. Nucl. Fus. Res., 1, 69-80 (IAEA, Vienna, 1969)
- de Hoffman, F., Teller, E., Phys. Rev., 80, 692-703 (1950)
- Holzer, R. E., McCleod, M. G., Smith, E. J., J. Geophys. Res., 71, 1481-86 (1966)
- Inoue, Y., J. Phys. Soc. Japan, 25, 881-887 (1968)
- Inoue, Y., J. Phys. Soc. Japan, 26, 521-528 (1969)
- Jackson, J. D., Plasma Phys. (J. Nucl. Energy, Part C), 1, 171-189 (1960)
- Kadomtsev, B. B., Plasma Turbulence (Academic Press, London, 149 pp., (1965)

- Kantrowitz, A. R. , Petschek, H. E. , MHD characteristics and shock waves.
 In Plasma Physics in Theory and Application, 148-206 (Kunkel, W. B. ,
 Ed. , McGraw Hill, New York, 494 pp. , 1966)
- Kellogg, P. J. , J. Geophys. Res. , 67, 3805-11 (1962)
- Kellogg, P. J. , Phys. Fluids, 7, 1555-71 (1964)
- Krall, N. A. , Book, D. L. , Phys. Fluids, 12, 347-355 (1969a)
- Krall, N. A. , Book, D. , Phys. Rev. Lett. , 23, 574-576 (1969b)
- Landau, L. D. , Lifschitz, E. M. , Fluid Mechanics, 342-344 (Addison-
 Wesley, Reading, Mass. , 536 pp. , 1959)
- Macmahon, A. B. , Bull. Am. Phys. Soc. , 13, 1518 (1968)
- Marshall, W. , Proc. Roy. Soc. Lond. , A233, 267-282 (1955)
- Ness, N. F. , Scarce, C. S. , Seek, J. B. , J. Geophys. Res. , 69, 3531-
 69 (1964)
- Neugebauer, M. , Snyder, C. W. , Science, 138, 1095-96 (1962)
- Olson, J. V. , Holzer, R. E. , Smith, E. J. , J. Geophys. Res. , 74, 4601-17
 (1969)
- Parker, E. N. , Astrophys. J. , 128, 664-676 (1958)
- Patrick, R. M. , Pugh, E. R. , Phys. Fluids, 10, 2579-85 (1967)
- Patrick, R. M. , Pugh, E. R. , Phys. Fluids, 12, 366-378 (1969)
- Paul, J. W. M. , Daughney, C. C. , Holmes, L. S. , Nature, 223, 822-824,
 (1969)
- Paul, J. W. M. , Holmes, L. S. , Parkinson, M. J. , Sheffield, J. , Nature,
208, 133-135 (1965)
- Paul, J. W. M. , Goldenbaum, G. C. , Iiyoshi, A. , Holmes, L. S. ,
 Hardcastle, R. A. , Nature, 216, 363-364 (1967)
- Petschek, H. E. , Rev. Mod. Phys. , 30, 966-974 (1958)
- Petschek, H. E. , AAS-NASA Symposium on the Physics of Solar Flares,
 425-439 (Hess, E. , Ed. , U. S. Govt. Printing Office, Washington, D. C. ,
 465 pp. , 1964) NASA SP-50
- Petschek, H. E. , Thorne, R. M. , Astrophys. J. , 147, 1157-63 (1967)

- Robson, A. E. , Sheffield, J. , Plasma Phys. and Contr. Nucl. Fus. Res. ,
1, 119-128 (IAEA, Vienna, 1969)
- Russel, C. T. , Olson, J. V. , Holzer, R. E. , J. Geophys. Res. , 73, 5769-
75 (1968)
- Saffman, P. G. , J. Fluid Mech. , 11, 16-20 (1961a)
- Saffman, P. G. , J. Fluid Mech. , 11, 551-566 (1961b)
- Sagdeev, R. Z. , Magnetohydrodynamic shock waves in low density gases.
Proc. Symp. Electromag. and Fluid Dyn. of Gaseous Plasma, 443-450
(Fox, J. , Ed. , Interscience, New York, 468 pp. , 1962a)
- Sagdeev, R. Z. , Sov. Phys. -Tech. Phys. , 6, 867-871 (1962b)
- Sagdeev, R. Z. , Cooperative phenomena and shock waves in collisionless
plasmas. In Review of Plasma Physics, 23-91 (Leontovich, M. A. ,
Ed. , Consultants Bureau, New York, 241 pp. , 1966)
- Sagdeev, R. Z. , On ohm's law resulting from instability. Proceedings of
Symposia in Applied Mathematics, 18, 281-286 (Grad, H. , Ed. , American
Mathematical Society, Providence R. I. , 293 pp. , 1967)
- Smith, E. J. , Holzer, R. E. , McCleod, M. G. , Russel, C. T. , J. Geophys.
Res. , 72, 4803-13 (1967)
- Spitzer, L. , Härm, R. , Phys. Rev. , 89, 977-981 (1953)
- Spreiter, J. R. , Jones, W. P. , J. Geophys. Res. , 68, 3555-64 (1963)
- Spreiter, J. R. , Summers, A. L. , Alksne, A. Y. , Planetary Space Sci. ,
14, 223-253 (1966)
- Spreiter, J. R. , Alksne, A. Y. , Ann. Rev. of Fluid Mech. , 2, 313-354
(1970)
- Storey, L. R. O. , Phil. Trans. Roy. Soc. Lond. , A246, 113-141 (1953)
- Stringer, T. E. , J. Nucl. Energy Part C, 5. 89-107 (1963)
- Stringer, T. E. , J. Nucl. Energy Part C, 6, 267-279 (1964)
- Tidman, D. A. , Phys. Fluids, 10, 547-564 (1967a)
- Tidman, D. A. , J. Geophys. Res. , 72, 1799-1808 (1967b)
- Woods, L. C. , Plasma Phys. , 11, 25-34 (1969a)
- Woods, L. C. , J. Plasma Phys. , 3, 435-447 (1969b)

Zagorodnikov, S. P. , Smolkin, G. E. , Sholin, G. V. , Soviet Physics JETP,
25, 783-789 (1967)

Zhigulev, V. N. , Romishevskii, E. A. , Soviet Phys. Doklady, 4, 859-862
(1960)

DOCUMENT CONTROL DATA - R&D

(Security classification of title, body of abstract and indexing annotation must be entered when the overall report is classified)

1. ORIGINATING ACTIVITY (Corporate author) Avco Everett Research Laboratory 2385 Revere Beach Parkway Everett, Massachusetts		2a. REPORT SECURITY CLASSIFICATION Unclassified	
		2b. GROUP	
3. REPORT TITLE COLLISIONLESS SHOCKS IN PLASMAS			
4. DESCRIPTIVE NOTES (Type of report and inclusive dates) Research Report 363			
5. AUTHOR(S) (Last name, first name, initial) Friedman, H. W. , Linson, L. M. , Patrick, R. M. and Petschek, H. E.			
6. REPORT DATE December 1970		7a. TOTAL NO. OF PAGES 37	7b. NO. OF REFS 80
8a. CONTRACT OR GRANT NO. F44620-70-C-0023		9a. ORIGINATOR'S REPORT NUMBER(S) Research Report 363	
b. PROJECT NO. 9752-02			
c. 61102F		9b. OTHER REPORT NO(S) (Any other numbers that may be assigned this report)	
d. 681308			
10. AVAILABILITY/LIMITATION NOTICES			
11. SUPPLEMENTARY NOTES		12. SPONSORING MILITARY ACTIVITY AF Office of Scientific Research, (SREP) 1400 Wilson Boulevard, Arlington, Virginia 22209	
13. ABSTRACT A review of experimental and theoretical work on shock waves in plasmas where classical collisions are unimportant is presented. The role of dissipation and dispersion in determining shock structure is described and several mechanisms which can provide the required dissipation in collisionless plasmas are discussed. Observations of collisionless shocks produced in laboratory experiments as well as the Earth's bow shock occurring naturally in space are described. Criteria are given when a shock may be considered thin so as to be treated as a discontinuity for flow field calculations. Experimental and theoretical areas where more work is needed are pointed out.			

14. KEY WORDS	LINK A		LINK B		LINK C	
	ROLE	WT	ROLE	WT	ROLE	WT
1. Collisionless shocks 2. Shocks 3. MHD shocks 4. Plasma turbulence 5. Collisionless dissipation						

INSTRUCTIONS

1. **ORIGINATING ACTIVITY:** Enter the name and address of the contractor, subcontractor, grantee, Department of Defense activity or other organization (*corporate author*) issuing the report.

2a. **REPORT SECURITY CLASSIFICATION:** Enter the overall security classification of the report. Indicate whether "Restricted Data" is included. Marking is to be in accordance with appropriate security regulations.

2b. **GROUP:** Automatic downgrading is specified in DoD Directive 5200.10 and Armed Forces Industrial Manual. Enter the group number. Also, when applicable, show that optional markings have been used for Group 3 and Group 4 as authorized.

3. **REPORT TITLE:** Enter the complete report title in all capital letters. Titles in all cases should be unclassified. If a meaningful title cannot be selected without classification, show title classification in all capitals in parenthesis immediately following the title.

4. **DESCRIPTIVE NOTES:** If appropriate, enter the type of report, e.g., interim, progress, summary, annual, or final. Give the inclusive dates when a specific reporting period is covered.

5. **AUTHOR(S):** Enter the name(s) of author(s) as shown on or in the report. Enter last name, first name, middle initial. If military, show rank and branch of service. The name of the principal author is an absolute minimum requirement.

6. **REPORT DATE:** Enter the date of the report as day, month, year; or month, year. If more than one date appears on the report, use date of publication.

7a. **TOTAL NUMBER OF PAGES:** The total page count should follow normal pagination procedures, i.e., enter the number of pages containing information.

7b. **NUMBER OF REFERENCES:** Enter the total number of references cited in the report.

8a. **CONTRACT OR GRANT NUMBER:** If appropriate, enter the applicable number of the contract or grant under which the report was written.

8b, 8c, & 8d. **PROJECT NUMBER:** Enter the appropriate military department identification, such as project number, subproject number, system numbers, task number, etc.

9a. **ORIGINATOR'S REPORT NUMBER(S):** Enter the official report number by which the document will be identified and controlled by the originating activity. This number must be unique to this report.

9b. **OTHER REPORT NUMBER(S):** If the report has been assigned any other report numbers (*either by the originator or by the sponsor*), also enter this number(s).

10. **AVAILABILITY/LIMITATION NOTICES:** Enter any limitations on further dissemination of the report, other than those

imposed by security classification, using standard statements such as:

- (1) "Qualified requesters may obtain copies of this report from DDC."
- (2) "Foreign announcement and dissemination of this report by DDC is not authorized."
- (3) "U. S. Government agencies may obtain copies of this report directly from DDC. Other qualified DDC users shall request through _____."
- (4) "U. S. military agencies may obtain copies of this report directly from DDC. Other qualified users shall request through _____."
- (5) "All distribution of this report is controlled. Qualified DDC users shall request through _____."

If the report has been furnished to the Office of Technical Services, Department of Commerce, for sale to the public, indicate this fact and enter the price, if known.

11. **SUPPLEMENTARY NOTES:** Use for additional explanatory notes.
12. **SPONSORING MILITARY ACTIVITY:** Enter the name of the departmental project office or laboratory sponsoring (*paying for*) the research and development. Include address.
13. **ABSTRACT:** Enter an abstract giving a brief and factual summary of the document indicative of the report, even though it may also appear elsewhere in the body of the technical report. If additional space is required, a continuation sheet shall be attached.

It is highly desirable that the abstract of classified reports be unclassified. Each paragraph of the abstract shall end with an indication of the military security classification of the information in the paragraph, represented as (TS), (S), (C), or (U).

There is no limitation on the length of the abstract. However, the suggested length is from 150 to 225 words.

14. **KEY WORDS:** Key words are technically meaningful terms or short phrases that characterize a report and may be used as index entries for cataloging the report. Key words must be selected so that no security classification is required. Identifiers, such as equipment model designation, trade name, military project code name, geographic location, may be used as key words but will be followed by an indication of technical context. The assignment of links, rules, and weights is optional.

DISTRIBUTION LIST
Contract F44620-70-C-0023

Stevens Institute of Technology, Dept. of Physics, Hoboken, New Jersey 07030, Attn: Dr. Winston H. Bostick (1 copy)

Space Technology Laboratories, TRW Systems, Inc., One Space Park, Redondo Beach, California 90278, Attn: Dr. C. L. Dailey (1 copy)

GEOTEL Inc., Plasmadyne Division, Santa Ana, California 92702, Attn: Mr. A. C. Ducati (1 copy)

Columbia University, Applied Science & Engineering Dept., New York, New York 10027, Attn: Dr. Robert A. Gross (1 copy)

University of Illinois, Dept. of Electrical Engineering, Urbana, Illinois 61801, Attn: Dr. C. D. Hendricks (1 copy)

Texas Technological College, Dept. of Electrical Engineering, Lubbock, Texas 79409, Attn: Dr. M. Kristiansen (1 copy)

AVCO Corporation, Avco Everett Research Laboratory, Everett, Massachusetts 02149, Attn: Dr. G.S. Janes (1 copy)

Ohio State University Research Foundation, Physics Department, Columbus, Ohio 43212, Attn: Dr. M. L. Pool (1 copy)

Stanford University, Mechanical Engineering Dept., Stanford, California 94301, Attn: Prof. Robert Eustis (1 copy)

AVCO Corporation, Avco Everett Research Laboratory, Everett, Massachusetts 02149, Attn: Dr. Richard M. Patrick (1 copy)

City University of New York, City College Research Foundation, New York, New York 10031, Attn: Dr. Norman C. Jen (1 copy)

United Aircraft Corporation, United Aircraft Research Laboratory, East Hartford, Connecticut 06108, Attn: Dr. Alan F. Haught (1 copy)

Stanford University, Dept. of Electrical Engineering, Stanford, California 94305, Attn: Dr. Donald A. Dunn (1 copy)

North Carolina State University, Physics Dept., Raleigh, North Carolina 27607, Attn: Dr. Willard H. Bennett (1 copy)

University of Tennessee Space Institute, Dept. of Physics, Tullahoma, Tennessee 37388, Attn: Dr. John B. Dicks (1 copy)

University of Miami, Physics Dept., Coral Gables, Florida 33124, Attn: Prof. Daniel R. Wells (1 copy)

Mobil Oil Corporation, Central Research Division, Princeton, New Jersey 08540, Attn: Dr. Robert L. Hickok (1 copy)

President. STD Research Corp., Pasadena, California 91106, Attn: Mr. S. T. Demetriades (1 copy)

University of Toronto, Institute for Aerospace Studies, Toronto, Canada, Attn: Dr. R. M. Measures (1 copy)

University of Rochester, Dept. of Mechanical & Aerospace Science, Rochester, New York 14627, Attn: Dr. Moshe J. Lubin (1 copy)

University of Innsbruck, Institute for Theoretical Physics, Innsbruck, Austria, Attn: Professor F. Cap (1 copy)

Tel-Aviv University, Dept. of Applied Mathematics, Ramat-Aviv, Tel-Aviv, Israel, Attn: Dr. Nima Geffen (1 copy)

University of Illinois, Dept. of Electrical Engineering, Urbana, Illinois 61820, Attn: Dr. Joseph Verdeyen (1 copy)

Berkeley Analytical Sciences Service Inc., Box 1250, Berkeley, California 94701, Attn: Mr. John Wyatt (1 copy)

Massachusetts Institute of Technology, Dept. of Aeronautics & Astronautics, Cambridge, Massachusetts 02139, Attn: Dr. James McCune (1 copy)

Air-Vehicle Corporation, 8873 Balboa Avenue, San Diego, California 92123, Attn: Dr. Jan Roszczewski (1 copy)

General Electric Co., Valley Forge, Pennsylvania 19101, Attn: Dr. Charles S. Cook (1 copy)

U.S. Naval Postgraduate School, Physics Dept., Monterey, California 93940, Attn: Dr. Fred Schwirzke (1 copy)

University of California, Dept. of Electrical Engineering and Computer Sciences, Berkeley, California 94720, Attn: Dr. A. J. Lichtenberg (1 copy)

Case Western Reserve University, Cleveland, Ohio 44106, Attn: Dr. Sheldon Gruber (1 copy)

Case Western Reserve University, Director, Plasma Research Laboratory, Cleveland, Ohio 44106, Attn: Dr. Osman K. Mawardi (1 copy)

Greek Atomic Energy Commission, Nuclear Research Center, Aghia Paraskevi, Attikis, Athens, Greece, Attn: Dr. A. Anastasiades (1 copy)

Carnegie Mellon University, Dept. of Electrical Engineering, Pittsburgh, Pennsylvania 15214, Attn: Dr. John G. Siambis (1 copy)

Office of Naval Research, Dept. of Navy, Power Branch (Code 429), Washington, D. C. 20360, Attn: Commander Gayland J. Mischke (1 copy)

Office of Naval Research Branch Office, Box 39, Fleet Post Office, New York, New York 09510, Attn: Commander Officer (1 copy)

Naval Research Laboratory, Director, Technical Information Division, Washington, D. C. 20390, Attn: 2027 (1 copy)

Mr. Frank J. Mollura, Rome Air Development Center, Griffiss AFB, New York 13440, Attn: EMEAM (1 copy)

Frank Shields, U.S. Army Mobility Equipment Research & Development Center, Fort Belvoir, Virginia 22060, Attn: SMEFB-EA (1 copy)

NASA Lewis Research Center, 21000 Brookpark Road, Cleveland, Ohio 44135, Attn: Dr. B. Lubarsky, Chief, Space Power Systems Division (1 copy)

AFOSR (SREP), 1400 Wilson Boulevard, Arlington, Virginia 22209 (25 copies)

Headquarters NASA (OART), Washington, D. C. 20546, Attn: Mr. J. Mullin (1 copy)

European Office of Aerospace Research, APO New York 19667, Attn: Lt. Col. Richard Boverie (ERTE) (1 copy)

AF Rocket Propulsion Laboratory (RPRE), Edwards AFB, California 93523, Attn: Mr. Clifford Hurd (1 copy)

AF Aero Propulsion Laboratory, Wright-Patterson AFB, Ohio 45433, Attn: Robert Cooper (APIE-4) (1 copy)
Mr. Philip Stover (APIE) (1 copy)
Mr. Robert Johnson (APIE-2) (1 copy)

National Science Foundation, Physics Section, Atomic & Molecular Physics, 1800 G Street, N.W., Washington, D. C. 20550, Attn: Dr. Sinclair (1 copy)

L. G. Hanscom Field, Branch Chief (AFCRL/CREA), Bedford, Massachusetts 01731, Attn: Dr. Morton Levine (1 copy)

Aerospace Research Laboratories, Wright-Patterson AFB, Ohio 45433, Attn: Colonel William K. Moran, Jr. (3 copies)

Hq AFSC (SCTSP), Andrews AFB, D. C. 20331, Attn: Major B. W. George (1 copy)

ARL (ARD-1), Wright Patterson AFB, Ohio 45433, Attn: Dr. Hans Von Ohain, Chief Scientist (1 copy)

U.S. Atomic Energy Commission, Research Division, Washington, D. C. 20545, Attn: Dr. R. Gould (1 copy)

NASA-Lewis Research Center, Propulsion Division, 21000 Brookpart Road, Cleveland, Ohio 44135, Attn: Wolfgang E. Moeckel (1 copy)

U.S. Atomic Energy Commission, Research Division, Washington, D. C. 20545, Attn: Dr. Robert Hirsch (1 copy)